

RAPID DESIGN, FABRICATION AND OPTIMIZATION OF A SINGLE EVENT THERMO-PNEUMATIC MICROACTUATION FOR THE DELIVERY OF MINUTE AMOUNTS OF LIQUIDS

Andres M. Cardenas-Valencia, cardenas@marine.usf.edu, David P. Fries, dpfries@marine.usf.edu, Larry C. Langebrake, llange@marine.usf.edu, Robert F. Benson, rbenson@marine.usf.edu

Center for Ocean Technology, 140 Seventh Ave N. St. Petersburg, FL,
USA, 33701

ABSTRACT

The need for efficient metering control of liquids in small devices has led to a boom in the advent of different micro-fluidic actuation mechanisms. Here we present a brief study on a thermal-pneumatic actuation mechanism for an on-demand delivery of minute amounts of liquids. A closely coupled, iterative design-fabrication strategy is used for optimization of a system in which no freely moving membranes are included. Special consideration was given to the heating device, minimizing the energy consumed. The fabrication method and performance of two types of fabricated resistors are compared herein. The first, a conventional Nickel-Chromium resistor using, lift-off micro-fabrication techniques, was initially tested. The second, a Copper clad liquid crystal polymer in conjunction with a novel mask-less patterning system was used to produce non-conventional heating micro-ohmic heaters. The heating efficiency was proven to be superior using the latter approach. Various micro-fabricated fluidic devices have been designed as case studies and have been fabricated and integrated using a variety of materials to illustrate the functionality of the approach. The combination of design and fabrication steps, the simplicity of the resistive device, and the materials selected combined, yield a direct path to making fluidic transport devices for micro-analytical and power systems.

INTRODUCTION & RATIONALE

The introduction of micro-electro-mechanical systems, (MEMS) devices in the biomedical and analytical chemistry arenas has increased the demand for efficient and

reliable micro-fluidics systems. Analysis in small-sized devices offers the potential for a reduction of reagents, time and cost. In order to achieve higher reliability in these small devices proper design of micro-channels distribution is needed, while precisely controlling the pumping and actuation of fluids. As pointed out by Rem et al (2001) controlled metering or single event delivery of discrete amounts of liquid is fundamental in complex analytical schemes. Metering, involves the coordination of pumping and valve actuation of a working fluid. A number of pumping mechanisms have been reported and evaluated (van den Berg and Lammerick, 1998; Shoji, 1998). Electro-kinetic, methods such as electro-dynamic and electro-osmosis, suffer from dependence on the electrical properties of the solution that is to be transported. Another drawback of relying on the electric nature of the fluid for actuation is that they restrict the wiring and electric interfacing of other devices in complex systems. Due to the disadvantages of electro-kinetic systems, pneumatic mechanisms are generally preferred (Lee and Kim, 2001). However, Direct interfacing of the micro-channels with peripheral pressure/vacuum plugs, is an option that will be difficult to implement in devices that constitute a portable system. An alternative is presented by the use of piezoelectric membranes that, however, require large voltages even though the currents are relatively low. The high heat exchange in small devices makes thermal initiation an attractive option. Thermal generation of pressure gradients, due to phase change, has been the principle used for design of several micro-valves (Henning 1998) and micro pumps (Maghribi et al, 2001). An alternative to creating a stroke arising from the phase change due to the vaporization of fluid is to use fluid expansion, due to heating. In the published designs relatively large head pressures, and wide operation ranges, are sought (Richter et

al, 1998 and Shoji, 1998). Low energy power is normally ignored since, in most cases, a continuous usage micro-pump is the major objective. A variety of control methods for micro fluidic valve designs are available. Several combinations of the different micro-fluidic functions have been integrated successfully. One example of such integration is the CD-like biomedical analysis platform (Madou et al, 2001). The metering is achieved by using capillary burst valving. A reservoir will deliver liquid to a channel when, due to the spinning, the centrifugal forces overcome the capillary restriction. The spinning is achieved through an external rotor. The use of capillary forces to induce and restrict flow (capillary burst valves) has become widely exploited in other micro fluidic devices (Lee and Kim, 2001; Tas et al, 2002).

In order to develop a simple to manufacture and robust, minimal-power micro-fluidic delivery mechanism, an electrical heater based thermal-pneumatic actuation was chosen. The heater will increase the temperature of a working fluid and a solution, placed next to the working fluid, will be pushed into a micro-fluidic channel when the expansion of the working fluid takes place. This concept has been presented previously as a means to initiate electrochemical micro-power devices (Cardenas-Valencia et al, in press). In that case both the working liquid and the solution to be actuated were contained in the same reservoir. Herein we have expanded the concept to placing these liquids in different connected reservoirs. Capillary stops will be used to interconnect the micro-fluidic paths. However a detailed discussion on the design of these will not be reported herein due to space limitations. In this paper, the design steps, with special consideration to optimizing the electrical heating and the actuation time, will be outlined. In the reference by Cardenas-Valencia et al (in press) two types of micro-fabrication techniques are used for the resistor fabrication. The first comprises the use of standard Nickel Chromium deposition on silicon wafers. The second, Copper resistors (Tin-plated to protect from corrosion), were made using non-conventional micro-fabrication techniques. In this case, popular materials in printed circuit board (PCB) technology were used. Recently, the use of traditional PCB technology materials has appeared in the micro-fabrication arena and several micro-fabricated devices using these materials have been reported (Merkel et al, 1998; Nguyen and Huang, 2001). Additionally, the moisture resistance properties of the substrates used here, have allowed them to become the materials of choice for packaging and enclosure of MEMS devices (Yang, 2002). The non-conventional fabrication of resistors is also unique since it used a mask-less lithographic photo-resist/etching/developing process. The combination of these features enables a less complex fabrication scheme when compared to standard micro-fabrication processes. In this manuscript, we will detail the performance and characterization of the heating devices and a simple coupled design-fabrication protocol with the goal of optimizing the heating of the working fluid. As an example, an actuated micro-fluidic cell has been assembled and tested.

CONSIDERATIONS FOR THE MICROFLUIDIC DESIGN

Working liquid selection

Saturated fluorocarbons, ($C_nF_{(2n+2)}$), are used as a solvents in thermal management applications. 3M Corp. markets some of these compounds under the name "FluorinertTM". They exhibit low viscosity, zero ozone depletion potential, non-toxicity, non-flammability, and their non-conductivity. We have decided to use the 3M-compound named FC-77 due to its outstanding thermodynamic properties. It poses a high coefficient of expansion, (β) and its heat capacity value, (C_p) is also considerably less than that of water. ($\beta = 0.0014 \text{ K}^{-1}$ and 1.170 J/g-C at 25 C (3M Specialty Materials, 1999)). Additionally, it is immiscible with water rendering a bi-phase system with the capacity to mechanically push aqueous solutions upon single phase expansion without the use of membranes. Also, with a boiling point of 97° C at 1 atm. (3M Specialty Materials, 1999), FC-77 can potentially be used in a broad range of working temperatures as working fluid for water solutions.

Conceptual design

In order to determine if the described approach will provide a reliable alternative to meter fluids, recall the isobaric thermal expansion equation for liquids

$$\Delta V = \beta V \Delta T \quad (1)$$

where ΔV is the change in volume and ΔT is the temperature increment experienced by the fluid. From this equation it seems reasonable to believe that the fluidic stroke of amounts of liquids to be moved will be that of the working liquid expansion. However, when dealing with small flow channels of liquids it is known that capillary action can induce flow initiation. The choice of adequate materials could potentially lead to an interfacial tension of the liquid under interest that, in turn, can ease the filling of a channel or reservoir. In this sense the capillary restriction and the forming walls of the micro-channel are part of the pumping system because they contribute to the filling of a rectangular channel. The influence of the fabrication materials has been reported before (Man et al, 1999). Since the focus of this paper was to optimize the thermal-actuation, details on the interfacial forces and its contribution are not analyzed herein. This section will outline thermodynamically the potential initial pressure heads that can be produced for pushing a liquid with our proposed micro-fluidic design.

Potential pneumatic push. As explained previously, the internal pressure generated in the working fluid compartment will lead to the initiation of the flow. Theoretically, a pressure differential change as function of temperature, (T) and volume (V) is given by

$$dP = (\partial P / \partial T)_V dT + (\partial P / \partial V)_V dV \quad (2)$$

Since the volume will be kept constant we need to find the

coefficient $(dP/dT)_V$ in order to be able to quantify the pressure available to overcome the capillary restrictions. This coefficient could be calculated based on measurements of pressure increments as the temperature is raised in a constant volume recipient, and obtaining the derivative numerically. Alternatively, we can obtain $(dP/dT)_V$ with Euler chain rule

$$\left(\frac{\partial P}{\partial T}\right)_V = -1/\left[\left(\frac{\partial V}{\partial T}\right)_P \left(\frac{\partial V}{\partial P}\right)_T\right] = -\left(\frac{\partial V}{\partial T}\right)_P / \left(\frac{\partial V}{\partial P}\right)_T \quad (3)$$

Now, recall the definitions of the isothermal compressibility, (κ) ; and the isobaric thermal expansion coefficient:

$$\kappa = -(1/V)\left(\frac{\partial V}{\partial P}\right)_T \quad (4)$$

$$\beta = (1/V)\left(\frac{\partial V}{\partial T}\right)_P \quad (5)$$

thus, we obtain the coefficient, $(dP/dT)_V$ as;

$$\left(\frac{\partial P}{\partial T}\right)_V = -\beta/\kappa \quad (6)$$

β is reported by 3M (3M Specialty Materials, 1999) for FC-77, however, as is the case for a number of organic liquids, the compressibility is not reported (Garvin, 2002). In order to have an idea of the internal pressure we calculated the value of κ using two routes. Using the data provided by 3M, κ was obtain as function of temperature. For comparison purposes, we have calculated the value κ using the Lee-Kesler (1975) equation of state, which is known to be adequate for non-polar hydrocarbons. Temperature dependent values of $(dP/dT)_V$ were calculated using equation 6 and were fitted to a linear form leading to the expressions given in 7 and 8.

$$\left(\frac{\partial P}{\partial T}\right)_V [\text{bar/K}] = -.0400(T) + 21.02 \quad (7)$$

$$\left(\frac{\partial P}{\partial T}\right)_V [\text{bar/K}] = -.0418(T) + 18.44 \quad (8)$$

Due to the values used for the κ calculations, equation 7 and 8 are restricted to pressure and temperature conditions of 0.1 to 8.0 MPa, 300 to 370 K and from 0.1 to 0.5 MPa, 298 to 348 K, respectively. Pressure increments were calculated, by integrating the regressed equations (7) and (8) and are presented in figure 1.

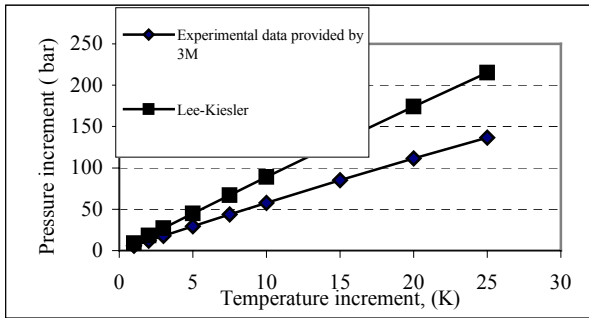


Figure 1. Potential initial pressure increments obtained by heating FC-77 in a reservoir due to heating.

Temperature rise: Modeling the heating efficiency. In order to theoretically quantify the amount of energy that is necessary to obtain a discrete expansion in the working fluid, it was necessary to characterize the heating of the

liquid. This could then be used to optimize the heating device, and ultimately, the micro-fluidic actuation. The following equations could be proposed to model the heating of the working fluid.

$$mCv(dT/dt) + UA(T - T_{\text{ext}}) = P_e \quad (9)$$

$$T = (P_e / UA) (1 - e^{-\frac{UA}{mCv}t}) + T_{\text{ext}} \quad (10)$$

These equations assumed that, for a constant input power, (P_e) the energy losses in the system could be represented by a constant overall heat transfer coefficient (U) , from the reservoir to its surroundings. The other variables are defined as follows: m is mass of FC-77; T_{ext} is the surroundings temperature. T_{ext} is also initial temperature of the working fluid, and t is the time required to reach T . The heat losses to the environment take place through an assumed area, A .

An alternative approach is to assume that, for a given resistor and input power, the instantaneous increment in temperature, dT , with respect to time, t is proportional to the amount of energy used, Win .

$$dT/dt = aWin \quad (11)$$

Regardless of the form in which the temperature increases, in order to assess the heating efficiency of the micro-fabricated heating device, a theoretical energy requirement to cause an increment in temperature can be calculated through thermodynamics. Since the working liquid is confined in a reservoir of constant volume, the heat capacity, Cv , is necessary. However, the Cv of liquids is not generally known. We calculated the value Cv based on the thermodynamic relationship, defining the difference between the specific heats:

$$C_p - C_v = (\beta^2/\kappa)TV \quad (12)$$

C_p , V and β , have been calculated using linear fit of data taken from 3M Specialty Fluids (1998) product literature. Values of κ , calculated as a function of T , were obtained as described before using two routes: The Lee-Kesler equation of state, and experimental data. In this manner two expressions for $Cv(T)$ were obtained, by using least squares linear regression;

$$Cv[\text{J}/(\text{kgK})] = 1.88(T) + 352.32 \quad (13)$$

$$Cv[\text{J}/(\text{kgK})] = 1.63(T) + 551.26 \quad (14)$$

MICROFABRICATION

The assembly procedure of the test micro-fluidic cells has been previously reported. Several layers were patterned with cavities that, when stacked, formed the three-dimensional micro-fluidic delivery system, (Cardenas-Valencia et al, in press). The channels fabrication was also conformed by PDMS elastomer. The fabrication of micro-fluidic devices using PDMS is well documented (Duffy et al, 1998; Jo et al, 200). The bonding of the layers was also achieved by in-situ polymerization of resin applied between the layers. The previously designed micro-fluidic cells had a single reservoir (in which both the working and the liquids actuated-to-be were in direct contact), and a rectangular

channel to fill. The design has been modified to a double reservoir (one for the working fluid and another for the actuation liquid) and a triangular cavity that is to be filled as a result of the actuation. The present design was based on our previous observations and simulation work. Figure 2 and Table 1 describe the stacked materials and dimensions of the layers involved in the cell fabrication.

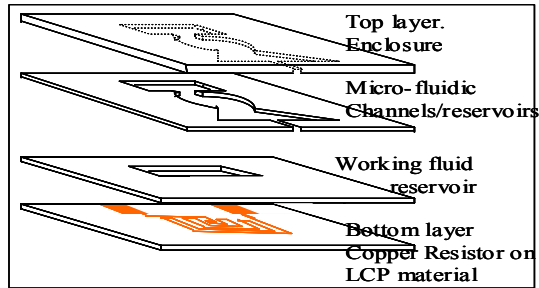


Figure 2. Isometric view of the thermo-pneumatic actuated micro-fluidic cell.

Table 1. Layers of the test micro-fluidic cell.

Layer	Material	Fabrication/Dimensions
1. Bottom	Cu Resistor/ LCP	Maskless Lithography. 9 μm Cu and 50 μm (0.002 in) LCP thickness
2	Working fluid reservoir	Fabricated by spin coating of PDMS resin. 500 μm depth.
3	Micro-channels	Fabricated by spin coating of PDMS resin. Height of channels= 80 μm
4. Top	PMMA/ Soft glass/ PDMS	Machined/Etched/Cast Approx 300 μm

Resistor micro-fabrication

Masking is one of the essential steps in micro-fabrication. Detailed processes for mask fabrication can be found elsewhere, (Gad-el-Hak, 2001) and it is commonly accepted that this process constitutes one of the most expensive and time-consuming tasks associated with the manufacture of micro-devices. As a comparison a very thin Nickel-Chromium resistor was fabricated using conventional techniques, specifically a lift off process on a glassy wafer material (Cardenas-Valencia, in press).

Mask-less Lithography. The mask-less patterning system used has been termed Smart Filter Technology and is unique when compared to other common exposure methods, (Hand, 2001). This micro-fabrication, Smart Filter Technology, contains the optics, light source, and integrated electronic components used to directly generate patterns for the exposure of photo-sensitive materials such as photo-resists and polymers. The equipment used was a model SF-100 (acquired from Intelligent Micro Patterning LLC, St Petersburg FL). The system is presented schematically in figure 3. The “artwork” or photo-image design is generated

in a computer using any available drawing software. The lines in figure 3 represent the image being transferred to the substrate. A microscope is used for substrate alignment with the pattern. The alignment is controlled through a computer controlled multi-axis stage that offers 35nm step sizes. Small opto-electronic components spatially modulate a high intensity light spectrum. Through the use of step indexing, multiple images can be shot on one substrate. The artwork pattern is then transferred to the substrate surface to expose the photosensitive material for the pattern transfer step. In this manner, quick and inexpensive patterning of different materials on other substrates can be achieved.

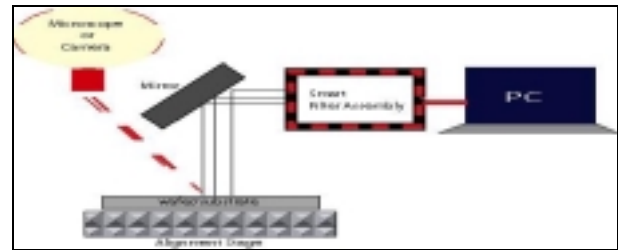


Figure 3. Maskless lithographic exposure workstation

A 13 μm copper-0.002” PCB flex-circuit material in which the substrate is a liquid crystal polymer (LCP), has been chosen. One of the major advantages of LCP materials is that it can be patterned with standard lithographic photo-resists and can be readily etched. The process flow for the micro-fabrication of resistors that will be used as heating devices is shown in figure 4. It is worth mentioning that the theoretical value of the designed resistors was in good agreement with the measured value. The Copper resistors were tin plated to protect the copper from oxidizing.

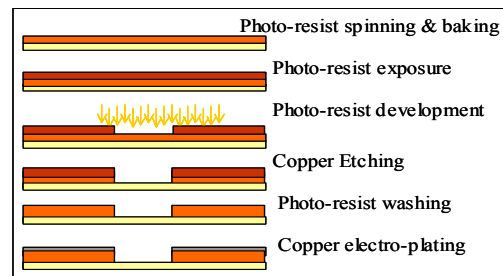


Figure 4. Process flow for the Copper/LCP resistors fabrication using mask-less lithography

TESTING PROTOCOL AND ITERATIVE DESIGN

In order to minimize the energy required initiating the micro-fluidic actuation, the resistor heating efficiency needed to be determined. Rather than taking a completely theoretical approach, it was decided to base the heater

characterization on experimental observation. Secondly the design of the resistor was optimized, by using thermal performance estimations and rapid prototyping of integrated micro-fluidics using micro-stereo lithography.

Characterizing the performance of the ohmic heaters

Required equipment. Temperature increments were measured using a HYPO-33 1T G 60 SMP M needle thermocouple and a DP460 Temperature display acquired from Omega Engineering. Voltages and current intensities applied were measured by means of Fluke-189 multi-meters.

Experimental protocol. Temperature vs time profiles at different electric power inputs were recorded for one of conventional and non-conventional micro-fabricated resistors. The information also helped to characterize the heating efficiency. Various micro-fluidic cells were assembled to test the heating efficiency. To perform the heating testing, only the 1st (bottom) and 2nd (FC-77 reservoir) layers, described in figure 1, were used. 80 micro liter reservoirs were prepared on the same substrates as the resistors. The area of these reservoirs was the same as described previously (Cardenas-Valencia, in press). A very thin PDMS layer was then glued to them and the temperature probe inserted through a small hole. The resistors were connected to a DC power source. The voltage, applied to the heating resistors, was varied and recorded several times in order to obtain temperature profiles. Figure 5 shows the temperature variation as a function of time for the Nickel-Chromium resistor and the Copper resistor 1 described in table 3.

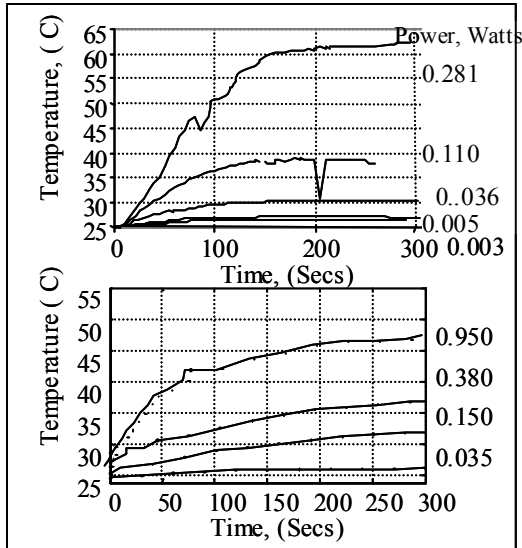


Figure 5. Temperature profiles as function of time for a Copper resistor, upper chart, (resistor 1 in table 3) and a Nickel-Chromium resistor, lower chart, are shown at different power inputs

The results, in Fig. 5, reveal that the non-conventional resistors on LCP material provide a more viable alternative

for heating the FC-77 when compared to the fabricated Nickel Chromium in a Silicon wafer. Notice that the LCP-Copper resistor provides a significantly better heating device, since it provides steeper and faster temperature increments for any given power. These types of resistors will be used for the integration of the micro-fluidic test cell.

After deciding on the type of resistors to use to assemble a micro-fluidic test cell, selection of the optimal input power occurred next. The shape of the temperature profile suggests that a mathematical description in equations (9) and (10) could be adequate. In order to confirm this assumption, the product UA was calculated for both resistors as function of temperature. The values UA were found by fitting the experimental values of the temperature vs time to a form of equation (10). The regressed product UA at different temperatures for the Nickel-Chromium and the Tin-plated-Copper micro-resistors are presented in table 2. Table 2 reveals that the regressed UA values are a very strong function of temperature. This represents a very serious deviation to the assumptions made when the equations (9) and (10) were postulated. Based on this, it was decided to characterize the heating efficiency by using an expression of the form of equation (11).

Table 2. Comparison of the regressed values of UA for the conventional and Copper-LCP resistors

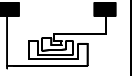


Nickel-Chromium resistor		Resistor 1	
Time (s)	UA, (J/ Ks)	Time (s)	UA, (J/ Ks)
26	22.5	26	0.004
28.25	6.923077	28.35	0.006
31.1	3.688525	32.55	0.007831
37.5	1.8	49.5	0.008733

Optimization of the Resistor through rapid fabrication.

Once we proved that a faster and more dramatic temperature change could be obtained using the LCP material, an optimization of the resistor design was sought. In this section we will outline the thought process for the optimization of the heating device. Optimization of the heater using this material could be achieved by changing the length and shape of the resistor. If, for a given power, the resistance (and length) of a heating device is increased with the same volume of heating fluid, a faster heating of the working fluid (FC-77) should be achieved. Basically, more energy will be exchanged to the working fluid because the energy input is more uniformly distributed in the heating surface. The fabricated resistors shapes are presented in table 3 together with data on the increment achieved at a given time. The input energy was calculated as follows;

$$W_{in} = \int_{t_1}^{t_2} P_e dt = \int_{t_1}^{t_2} (IV_e) dt \quad (15)$$

Table 3. Performance and resistor design obtained with the Cu-LCP mask less produced resistors.

Resistor	1	2	3
ΔT (K)	9.1	20	33
Time (s)	77	59	43
Power (W)	0.11	0.20	0.26
Energy (J)	9.1	11.7	14.0
Resistance	0.99	3.47	4.00
Artwork			

Assuming that an expression of the form of equation (11) is valid for a given power, allow us to write the temperature increment as function of time as a linear function. This is in fact the case for a wide range of time as revealed by the curves represented in figure 5. Least squares linear regression was performed for the curves of temperature increment vs time for the power applied up to 80 seconds. Slopes and the R^2 coefficient of the linear fits are reported for the different powers utilized in table 4.

Table 4. Power input and slope of the curves ΔT vs t for data obtained up to 80 seconds with resistor 1.

Run	Power input (W)	Slope, $(\Delta T)/t$, ($^{\circ}\text{C/s}$)	R^2
1	0.0025	0.018889	0.9927
2	0.005	0.022915	0.9913
3	0.036	0.054807	0.9863
4	0.1099	0.135035	0.9952
5	0.2805	0.29984	0.9931

It could be hypothesized that the increment in temperature vs power is maintained constant even if the resistor design is changed. If this is so, it should be possible to predict the curves of energy vs temperature within the linear temperature range, based only in only one experimental measurement. To test the validity of the assumption the values of $\Delta T/\Delta t$ vs power for the runs performed with resistor 1, and the single run of resistors 2 and 3, are plotted in Fig. 6.

The fact that the data of $\Delta T/\Delta t$, obtained with the three resistors fell close to a straight line, supports that a single point could be use to characterize the heating capability of a given resistor, regardless of the power used. Using this observed point of ΔT at the given time let us write for resistor 2 and 3, (Eqs. 16 & 17, respectively)

$$\Delta T = 1.71W \text{in} \quad (16)$$

$$\Delta T = 2.35W \text{in} \quad (17)$$

If our assumptions made to postulate that equations (16) and (17) were valid, regardless of the power, then we could predict the actual temperature increment.

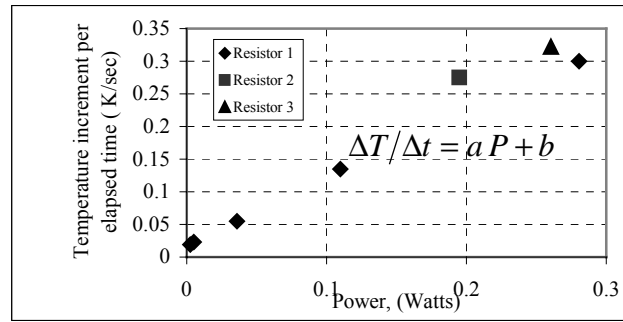


Figure 6. Temperature increment over time vs the power consumed for the three Copper-LCP resistors.

In order to corroborate this, more experimental runs with the three resistors were performed as described earlier, using different voltages (and power inputs). The actual temperature increments have been plotted against the prediction based solely on equations 17, 18. The agreement between the experimental and the calculated values using those equations is excellent. This proves that only one measurement was enough for the improved resistors designed. By, using equations (16) and (17) together with the data contained in figure 6, not only the temperature increment but also the time to reach certain temperature can be predicted for these three resistors.

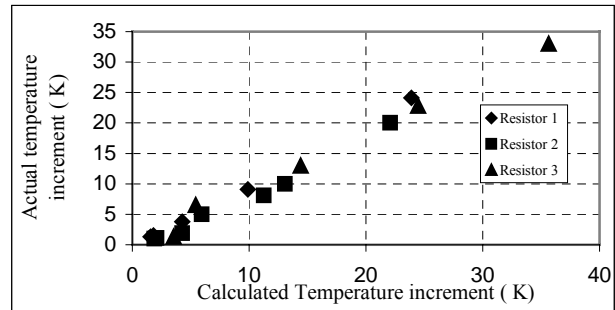


Figure 7. Actual vs Predicted temperature increments based on equations (16) and (17), for the resistors 1 2 and 3, after times of 80, 56 and 43 seconds, respectively

RESULTS AND DISCUSSION

Heating efficiency and Pressure head achieved.

The results presented above indicate that the higher resistance in resistors 2 and 3 confers a faster and more efficient heating input to the liquid in the reservoir. This is further confirmed by Figure 8, which shows the experimental temperature increments as function of energy for resistors 1,2 and 3 after approximately 80, 55 and 40 seconds, respectively.

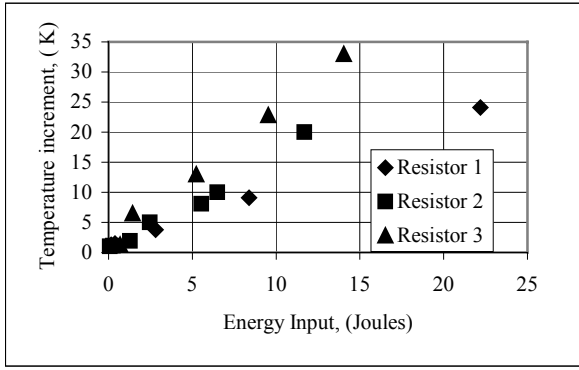


Figure 8. Experimental values obtained for the three different resistor designs.

Figure 8 confirms that the resistor design has an effect on its heating capability. Resistor designs 2 and 3 produce the highest heating input. This is in agreement with the fact that its contact surface area is the highest and more uniformly distributed on the bottom of the pit as was illustrated in table 3. Figure 8 shows that we have effectively been able to optimize the heating of the FC-77, establishing the basis for a more efficient micro-fluidic cell. An energetic heating efficiency can be obtained as a function of time by defining the following ratios, for calculations at constant pressure, Eq. (18) of at constant volume, Eq. (19).

$$(H.E.)_p = \frac{\int mC_p dT}{\int P_e dt} \quad (18)$$

Or
$$(H.E.)_v = \frac{\int mC_v dT}{\int P_e dt} \quad (19)$$

Based on Equations (18) and (10), one may think that the maximum efficiency will be achieved by the use of either small power (or voltage applied) or very short time applications. This statement, as proven by the provided results, is misleading since each power used has a maximum ΔT associated with it. So, for a given resistor the optimal power will have to be decided within the framework of a practical time necessary to reach a significant temperature increment. Table 5 summarizes the heating efficiency, indicating also the achieved temperature delta, as well as the power employed for all the experimental runs performed for the optimized fabricated resistor 3. Additionally, the last column provides the theoretical pressure head, that could have achieved for flow initiation, by constricting FC-77 into a reservoir when heated to the given temperature increment. From the provided analysis, it can be deduced that for a given resistor and at a given time different temperature delta are reachable depending on the electrical power imposed to the resistor. This would lead to broad range of different pressure gradients that are potentially attainable at different times depending on the pressure required to initiate the flow actuation. Increased efficiencies in the heat transfer has been achieved by using the rapid mask less-PCB approach described.

Table 5. Heating efficiencies calculated for several runs using resistor 3.

Power (W)	Time (s)	ΔT (K)	H. E. (%)	ΔP calculated (bars). Average of Eqs. (7) and (8)
0.016	43.2	1.3	17.64	9.77
0.032	45.5	6.5	42.03	48.16
0.116	45.3	13	23.40	94.59
0.226	42.2	21	20.95	149.36
0.260	53.9	34	23.30	232.78

Filling channels and reservoirs

The micro-fluidic thermal actuation to fill a channel and the triangular reservoir of an assembled cell has been successfully tested. The optimal voltage, to be applied to the resistors, was calculated based on the earlier reported results. For the cell assembled using resistor 3 a potential of 0.5 V was applied, (average power input was around 0.063 watts). In this case the amount of energy for such an actuation was found to be 2.5 Joules for the glass substrate and 2.0 Joules for the PMMA top most layer. For these cases, it approximately took half a minute after activation, for the aqueous solution to fill the triangular channel entirely. In order to establish the channel flow in the PDMS channels a higher voltage had to be applied. This indicates that hydrophobic/hydrophilic surface effects influence the capillary action and affecting the micro-fluidic actuation and the actuation energy.

CONCLUSIONS

An analysis for the design and construction of micro-fabricated heaters as part of a thermal-pneumatic micro-fluidic single event actuation scheme is discussed in this paper. The performance between a Nickel-Chromium and a Tin-plated-Copper on a liquid crystal polymer substrate were compared within. The performance of the latter suggested its use for a thermal pneumatic micro-fabricated cell. A simple and effective resistor characterization procedure was described. In addition, a protocol based on the simplified considerations was established to optimize the resistor performance. This in turn has rendered a smaller energy input for the micro-fluidic actuation. The simplicity of the described approach is enhanced by the use of a mask less lithography process on PCB materials. The mentioned advantages of the micro-fabrication technique, together with its versatility make it ideal for first-time testing research purposes. The results provided herein, constitute the basis for fabricating relatively low power, versatile, robust, and conceptually simple family of micro-delivery systems for diverse applications.

ACKNOWLEDGMENTS

Distribution Statement 'A'. Approved for Public Release-Distribution Unlimited. The financial support for this project, provided by the U.S. Army, Space and Missile Defense command to the University of South Florida through grant DASG60-00-C-0089 is gratefully acknowledged.

NOMENCLATURE

β Isobaric expansion coefficient [1/ K]
 Δ Increment operator
 ∂ Partial derivative operator
 κ Isothermal compressibility, [1/bar]
 A Available area for heat exchange [m²]
 Cp Heat capacity at constant pressure [J kg K]
 Cv Heat capacity at constant volume [J kg⁻¹ K⁻¹]
 d Differential operator
 I Electrical current intensity [A]
 m Mass of fluorinert [kg]
 P Pressure [Bar]
 Pe Electrical Power [Watts]
 t Time [s]
 T Temperature [K]
 T_{ext} Ambient temperature, (assumed to be initial working fluid temperature) [K]
 U Overall heat mass transfer coefficient [J m⁻² s⁻¹ K⁻¹]
 V Volume [m³]
 V_e Electric potential [V]
 W_{in} Work input in the form of electrical energy [J]

REFERENCES

- 3M Specialty materials. 2000, Fluorinert™ Electronic Liquid, Product Information ,St. Paul, MN. pp. 1-4
 3M Specialty materials. 1999, Fluorinert™ Electronic Liquids, Application Information ,St. Paul, MN. pp. 1-7
 Cardenas-Valencia, A. M., Challa, V. R., Fries, D. P., Langebrake, L. C., Benson, R. F., Bhansali, S., A Microfluidic Galvanic Cell as an On-line Chip Power Source, *Sens. and Act. B.*, In Press.
 Duffy D. C., MacDonald J. C., Schueller J. A. and Whitesides G. M., 1998, Rapid Prototyping of Microfluidic Systems in Polydimethylsiloxane, *Anal. Chem.*, Vol. 70, pp. 4974-4984.
 Gad-el-Hak, M. 2001, *The MEMS Handbook*, CRC Press. Series for Mechanical Engineering.
 Garvin, J., 2002, Use the Correct Constant-Volume Specific Heat". *Chem. Eng. Prog.*, July 2002, pp.64-65
 Hand, A., 2001, Start-up Company Exploits Maskless Photolithography Technique, *Sem. Int.*, Vol. 24 No 9, pp. 44
 Henning, A., 1998, Microfluidic MEMS, *Proc. IEEE Aero. Conf. Pistacaway, NJ.*
 Jo B.H., Van Lerberghe, L.M., Motsegood, K.M., Beebe D.J, 2000, Three-dimensional micro-channel fabrication in polydimethylsiloxane (PDMS) elastomer, *J. Micro-electr.-mech. Syst.*, Vol. 9 Issue: 1, pp.76-81.
 Lee, B. I., and Kesler, M. G., 1975, A Generalized Thermodynamic Correlation Based on Three-Parameter Corresponding States, *AIChE J.*, Vol. 21, No 3, pp. 510-527.
 Lee, S.-H., Kim Y.-K., 2001, Metering and Mixing of Nanoliter liquid in the Microchannel Networks driven by fluorocarbon Surfaces and Pneumatic Control, *Proc. Of the μ TAS 2001 Symposium*, Monterey, CA, pp.205-206.
 Madou, M. J., Lee, L. J., Daunert, S., Lai, S. and Shih, C.-H., 2001, Design and Fabrication of CD-like Microfluidic Platforms for Diagnostics: Microfluidic Functions, *Biom. Microdev.*, Vol. 3, No. 3, pp.245-254.
 Maghribi, M. N., Krulevitch, P., and Hamilton, J. K., 2001, Microsyringe arrays in Poly(dimethylsiloxane), *Proc. Of the μ TAS 2001 Symposium*, Monterey, CA, pp.165-166.
 Man, P. F., Mastrangelo, C. H., Burns, M. A., and Burke, D. T., 1999, Microfabricated Plastic Capillary Systems with Photo-definable Hydrophilic and Hydrophobic Regions, *Proc. of the 1999 Transducers Conference*, Sendai, Japan, pp.1. -5.
 Merkel, T., Graeber, M., and Pagel, L., 1998 A new technology for fluidic Microsystems based on PCB technology, *Sens. and Act.*, Vol. 77, pp. 98-105.
 Nguyen, N., and Huang, X, 2001, Miniature valve less pumps based on printed circuit board technique, *Sens. and Act: A*, Vol. 88, pp. 104-111.
 Rem, J. E., Shepodd, T. J., and Hasselbrink, E. F., 2001, Mobile Flow Control Elements for High Pressure Micro-Analytical Systems fabricated using In-situ polymerization, *Proc. Of the μ TAS 2001 Symposium*, Monterey, CA, pp. 227-228.
 Richter, M., Linnemann, R., and Woias, P., 1998 Robust design of gas and liquid micropumps, *Sens. and Act.: A*, Vol. 68, pp. 480-486
 Shoji, S. Fluids for Sensors Systems. 1998 *Topics in Cur. Chem.*, Vol. 194 pp.
 Tas, N. R., Berenschot, J. W., Lammerink, T. S. J., Elwenspoek, M., and van den Berg, A., 2002, Nanofluidic Bubble pump Using Surface Tension Directed Gas Injection, *Anal. Chem.*, 2002, Vol. 74, pp. 2224-2227.
 Tuma, P. E., 2001. Private communication, 3M Center 236-2B-01, St. Paul, MN 55144 3M Chemicals
 van den Berg A., and Lammerink, T. S. J., 1998 Micro Total Analysis Systems: Microfluidic Aspects, Integration Concepts and Applications. *Topics in Cur. Chem.* Vol. 194.
 R. Yang, 2002, Liquid Crystal Polymers, *Adv. Pack. Mag.*, March 2002, pp. 17-22.